

Transformation of Ag Nanowires into Semiconducting AgFeS₂ Nanowires

Beniamino Sciacca¹, Anil O. Yalcin², Erik C. Garnett^{1*}

¹ Center for Nanophotonics, FOM Institute AMOLF, Science Park Amsterdam 104, 1098 XG Amsterdam, The Netherlands

² Kavli Institute of Nanoscience, Delft University of Technology, Lorentzweg 1, 2628 CJ Delft, The Netherlands.

Supporting Information Placeholder

ABSTRACT: We report on the synthesis of semiconducting AgFeS₂ nanowires, obtained from the conversion of Ag nanowires. The study of the conversion process shows that the formation of Ag₂S nanowires, as an intermediate step, precedes the conversion into AgFeS₂ nanowires. The chemical properties of AgFeS₂ nanowires were characterized by X-Ray Diffraction (XRD), Scanning Electron Microscopy (SEM) and Energy Dispersive X-Ray Spectroscopy (EDS) at intermediate steps of the conversion process, and show that the temperature at which the reaction takes place is critical to obtaining nanowires as opposed to nanotubes. Optical measurements on nanowire ensembles confirm the semiconducting nature of AgFeS₂, with a direct band gap of 0.88 eV.

Ternary I-III-VI₂ semiconductors are receiving increasing attention as promising materials for photovoltaics because of their large absorption coefficient, tunable direct band gap, high conversion efficiency and low toxicity.¹⁻⁶ Copper indium gallium selenide (CIGS) based solar cells with an efficiency of 21.7% have achieved the record efficiency for single junction polycrystalline material⁷. The outstanding conversion efficiency achieved by I-III-VI₂-semiconductor-based solar cells has motivated us to investigate materials with the chalcopyrite (CuFeS₂) structure,^{8,9} where the group III element is substituted with Fe.

Nanowire photovoltaics offer several advantages over thin film architectures including relaxation of lattice strain at heterojunction interfaces¹⁰⁻¹⁵ and strong absorption arising from tunable optical resonances.¹⁶⁻¹⁸ Nanoscale optical resonances maximize absorption in small volumes via antenna effects, which theoretically enables higher open circuit voltage and thus efficiency values, due to reduced bulk recombination and optical concentration.^{19,20} Furthermore, at the nanoscale certain chemical processes such as galvanic replacement,^{21,22} cation exchange²³⁻²⁷ and the Kirkendall effect²⁸⁻³¹ occur

much more readily, facilitating the synthesis of complex nanostructures.

AgFeS₂ (lenaite) has been recently proposed as a potential absorbing material for solar cells,³² and in the only report available in literature its band gap has been reported to be around 1.2 eV. However, to the best of our knowledge, the synthesis of only small AgFeS₂ nanocrystals (≈ 15 nm)³² or large microparticles⁹ has been reported thus far. In this work we demonstrate the synthesis of AgFeS₂ nanowires, via a solution phase conversion of metallic Ag nanowires into semiconducting AgFeS₂ nanowires. XRD, SEM and EDS characterizations give insight into the conversion mechanism. We also show optical absorption measurements to determine the band gap.

AgFeS₂ nanowire characterization

The route to obtain AgFeS₂ nanowires was adapted from the previously described synthesis of pure phase FeS₂ nanocrystals.³³ Briefly, AgFeS₂ nanowires were obtained by reacting Ag nanowires with iron chloride, sodium thiosulfate and thioglycolic acid in dimethyl sulfoxide (DMSO) and water at 150 °C.

A representative elemental distributions (Fe, S and Ag) in a AgFeS₂ nanowire measured by EDS is presented in Figure 1a. The full EDS spectrum is shown in Figure S1c. EDS show that substantial amounts of sulfur and iron are present in the nanowires, along with silver, and they are homogeneously distributed. This indicates that during the conversion process Fe and S diffuse within the nanowire. However, the SEM image in Figure 1a shows the presence of several crystallites in the nanowires, suggesting that they are not single crystalline as opposed to the Ag nanowires employed as precursor. The inset shows a selected area electron diffraction (SAED) pattern confirming the polycrystallinity of these nanowires. Due to the large nanowire diameter, the crystallite size is not entirely clear in transmission electron microscopy (TEM) images (Fig. S1). However, an

average crystallite size of 35 nm is obtained using the Scherrer equation (details in SI).

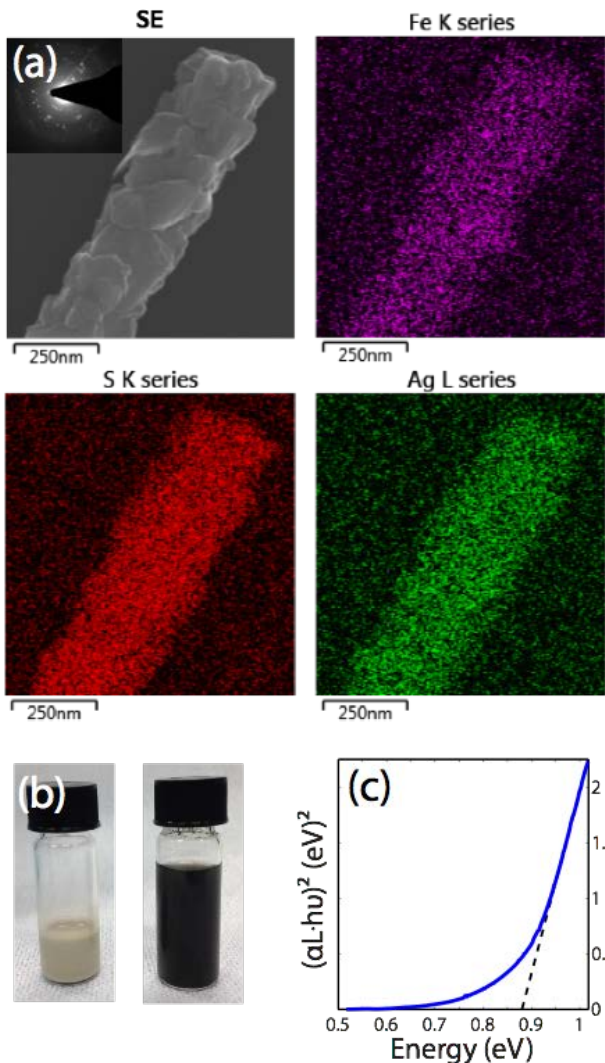


Figure 1: (a) EDS map of AgFeS₂ nanowires; the images show the chemical composition, highlighting the homogeneous element distribution within the nanowire; inset: SAED of AgFeS₂ nanowires; the image shows that the nanowires are polycrystalline. (b) optical images of dispersions of Ag (left) and AgFeS₂ (right) nanowires, showing the light absorption properties of AgFeS₂; (c) Band gap measurements of AgFeS₂ nanowire ensemble drop-cast from solution on a quartz slide; the direct optical transition is around 0.88 eV.

The change of the dispersion color from beige to black (Figure 1b) suggests the formation of a small band gap semiconductor after the conversion process, interestingly preserving the nanowire appearance. This is demonstrated in Figure 1c, that shows a Tauc plot of a AgFeS₂ nanowire ensemble deposited on quartz and measured between 0.5-1.2 eV. The linear relationship near the band edge indicates a direct band gap and the intercept value

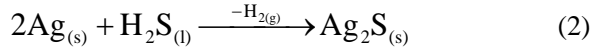
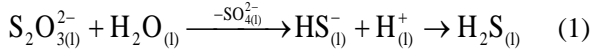
indicates a magnitude of 0.88 eV. Note that the sub-band gap absorption can either be caused by tail states or by the presence of an indirect transition at smaller energy. Considering the average crystallite size of 35 nm, quantum confinement effects can be excluded in our AgFeS₂ nanowires.

The band gap measured is lower than the value of 1.2 eV previously reported on small nanocrystals.³² The discrepancy in the band gap value measured for our AgFeS₂ nanowires compared to that measured for the 15 nm AgFeS₂ nanocrystals might be due to quantum confinement in the nanocrystals, although there is no report of the Bohr radius for this material. A Bohr radius as large as 10 nm, was previously reported for other chalcogenides materials such as CuInSe₂,³⁴ assuming comparable values for AgFeS₂, some weak quantum confinement in 15 nm nanocrystals could be expected. However, it is difficult to provide a conclusive explanation, considering the lack of reports in literature about the AgFeS₂ band gap.

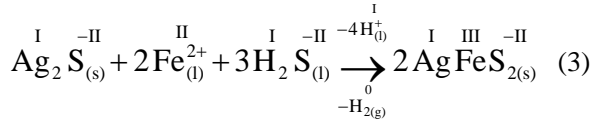
AgFeS₂ nanowire conversion process

The conversion of Ag nanowires into AgFeS₂ nanowires as a function of the reaction time and temperature was studied. Aliquots of the reacting solution were withdrawn at several time intervals and analyzed by EDS, XRD, and SEM. At $t=0$, i.e. after mixing the reagent together but before placing them in the heating bath, the nanowires present in the solution are pure crystalline Ag nanowires (Figure 2a,b); no other crystal phases are detectable in the XRD data, although negligible traces of sulfur were detected in the EDS spectrum of nanowires at $t=0$ (see Figure S1). This is probably due to residue from the solution, or to a thin amorphous silver sulfide layer. This suggests that no substantial sulfurization process takes place before heating. After 5 min Ag nanowires are fully converted to Ag₂S nanowires. This is supported by XRD measurements in Figure 2c, showing that the reflection peaks match with those of the achantite (Ag₂S) reference. The SEM image in Figure 2d displays the nanowire geometry of the sample after 5 min, showing changes in the morphology. In particular, a change in morphology is observed in some sections of the nanowires, because of the reorganization of the crystal structure from fcc (Ag) to monoclinic (Ag₂S). Note that at this stage of the conversion process, a small amount of a AgFeS₂ phase (peaks aligned with blue lines in Figure 2c) is already present in the sample; this is supported by traces of Fe in the EDS spectrum (see Figure S1). These findings suggest that the conversion of Ag nanowires to AgFeS₂ nanowires, goes through an intermediate step, where the formation of Ag₂S nanowires takes place at the very early stage ($t < 5$ min). Thiou sulfate disproportionation (Eq. 1)³⁵ leads to the for-

mation of H_2S , which sulfurizes Ag nanowires according to Eq. 2.



After the formation of Ag_2S nanowires, H_2S further reacts with Ag_2S and with Fe^{2+} cations, leading to the incorporation of Fe inside the nanowire structure. A possible reaction pathway is shown in Eq. 3:



No change in the oxidation states of Ag or S is occur-

ring in Eq. 3, which remain in the I and -II oxidation states respectively, consistently with what is observed in CuFeS_2 .^{36,37} Iron (II) is oxidized to Iron (III), with the concurrent reduction of hydrogen (Eq. 3). XRD data on nanowire ensembles drop-cast from solution after 90 min, are presented in Figure 2e, along with the reference pattern for AgFeS_2 , reported for comparison. The agreement between the reference pattern and the experimental spectrum is good, demonstrating a successful conversion of Ag nanowires into pure phase crystalline AgFeS_2 nanowires.

Note that the shape of the nanowires is preserved at the end of the conversion (Figure 2f), but the roughness of the final samples suggests polycrystallinity. This is consistent with what was observed after 5 min, probably due to the crystal reorganization during the conversion to Ag_2S in the intermediate step. Note that no significant changes in the XRD spectrum are observed after aging for over two months in ambient conditions (see Fig. S3).

Temperature effect on the conversion process

The effect of the reaction temperature on the conversion process was systematically studied as well, keeping the reaction time at 90 min. If the reaction temperature is too low ($T < 70^\circ\text{C}$), only a sulfurization of the outer surface of Ag nanowires occurs (see Figure S2). XRD measurements (Figure S2a) imply that the main crystalline phase present is Ag. However EDS shows that a small amount of sulfur is present in the nanowires (see Figure S2b). This suggests that a thin layer of Ag_2S may be formed at the outer surface of Ag nanowires, but not enough to give appreciable X-ray signal, or it could be in an amorphous phase. This is corroborated by the SEM image in Figure S2c, which shows that the surface roughness of the nanowires is increased as compared to freshly prepared Ag nanowires. No traces of Fe are present in the EDS spectrum, suggesting that higher temperatures are needed to promote the Fe incorporation within the nanowire structure. When the reaction is performed at intermediate temperatures ($70\text{-}120^\circ\text{C}$), a hollowing process takes place, leading to the formation of nanotubes, as shown in the back-scattered-electron SEM image in Figure S3a. This is probably due to the Kirkendall effect, that takes place when the solid-state diffusion rates of flowing inward and outward migrating species are different, resulting in a hollow structure.^{28,29}

The Kirkendall effect depends also on temperature, geometry and reagent concentration.³⁸⁻⁴⁰ In our case the disproportionation of thiosulfate occurs faster at higher temperature, leading to an increased concentration of the oxidizing agent (H_2S) and therefore to a larger inward flux. The faster reaction rate and the higher inward flux prevent hollowing at elevated temperatures.

The crystal phase of such nanotubes produced at lower temperatures is a mixture of Ag_2S and AgFeS_2 , as shown

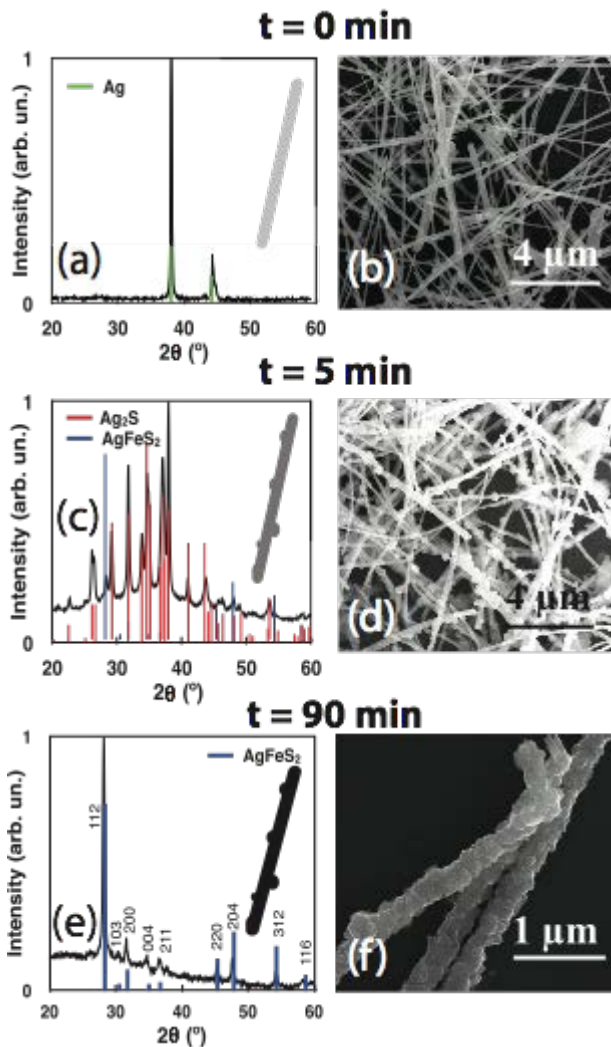


Figure 2: (a) XRD and (b) SEM measurements of an aliquot at $t=0$. (c) XRD and (d) SEM measurements of the Ag_2S intermediate ($t=5$ min). (e) XRD and (f) SEM of AgFeS_2 nanowires ($t=90$ min)

by XRD measurements in Figure S5b. No detectable crystal phase of Ag are present, consistent with migration and oxidation of the Ag core at the surface. EDS spectra confirm as well the presence of Ag, S and Fe in the nanotubes (see Figure S5c,d).

We have shown a novel synthetic pathway to obtain pure phase AgFeS₂ nanowires, employing Ag nanowires as the precursor. The reaction goes through an intermediate step during which Ag₂S nanowires are formed; during this phase the crystal structure undergoes a reorganization due to the different lattices, which produces polycrystalline nanowires. Ag₂S nanowires can then be converted into AgFeS₂ nanowires, keeping the same morphology. We have also shown that nanotubes with a mixed phase Ag₂S/AgFeS₂ can be prepared by performing the conversion process at a lower temperature. Ensemble optical absorption measurements show that AgFeS₂ nanowires have a direct band gap of approximately 0.88 eV, which is substantially lower than what was previously reported for AgFeS₂ nanocrystals. Given this band gap value, AgFeS₂ nanowires could be used for a variety of applications including multiple exciton generation, the bottom cell in a multi-junction solar cell, or the low-bandgap layer in a singlet-fission solar cell.

ASSOCIATED CONTENT

Supporting Information. Detailed methods, EDS of AgFeS₂ nanowires, Ag₂S nanowires, AgFeS₂ nanotubes are available. This material is available free of charge via the Internet at <http://pubs.acs.org>.

AUTHOR INFORMATION

Corresponding Author

*e.garnett@amolf.nl

ACKNOWLEDGMENT

The authors acknowledge AMOLF technical support, Dr. Bruno Ehrler, Dr. Sarah Brittan, for fruitful discussions. Furthermore we would like to acknowledge support from the Light Management in New Photovoltaic Materials (LMPV) center at AMOLF. This work is part of the research program of the Foundation for Fundamental Research on Matter (FOM), which is part of the Netherlands Organization for Scientific Research (NWO). The research leading to these results has received funding from the European Research Council under the European Union's Seventh Framework Programme (FP/2007-2013) / ERC Grant Agreement n. 337328, "NanoEnabledPV".

REFERENCES

(1) Yu, L. P.; Kokenyesi, R. S.; Kesler, D. A.; Zunger, A. *Advanced Energy Materials* **2013**, *3*, 43.

(2) Chirila, A.; Reinhard, P.; Pianezzi, F.; Bloesch, P.; Uhl, A. R.; Fella, C.; Kranz, L.; Keller, D.; Gretener, C.; Hagendorfer, H.; Jaeger, D.; Erni, R.; Nishiwaki, S.; Buecheler, S.; Tiwari, A. N. *Nature Materials* **2013**, *12*, 1107.

(3) Chirila, A.; Buecheler, S.; Pianezzi, F.; Bloesch, P.; Gretener, C.; Uhl, A. R.; Fella, C.; Kranz, L.; Perrenoud, J.; Seyrling, S.; Verma, R.; Nishiwaki, S.; Romanyuk, Y. E.; Bilger, G.; Tiwari, A. N. *Nature Materials* **2011**, *10*, 857.

(4) Huang, C.; Chan, Y.; Liu, F. Y.; Tang, D.; Yang, J.; Lai, Y. Q.; Li, J.; Liu, Y. X. *Journal of Materials Chemistry A* **2013**, *1*, 5402.

(5) Wang, D. S.; Zheng, W.; Hao, C. H.; Peng, Q.; Li, Y. D. *Chemical Communications* **2008**, 2556.

(6) Omata, T.; Nose, K.; Otsuka-Yao-Matsuo, S. *Journal of Applied Physics* **2009**, *105*, 73106.

(7) Jackson, P.; Hariskos, D.; Wuerz, R.; Kiowski, O.; Bauer, A.; Friedlmeier, T. M.; Powalla, M. *physica status solidi (RRL) – Rapid Research Letters* **2015**, *9*, 28.

(8) Boon, J. W. *Recueil des Travaux Chimiques des Pays-Bas* **1944**, *63*, 69.

(9) Galembeck, A.; Alves, O. L. *Journal of Materials Science* **1999**, *34*, 3275.

(10) Schoen, D. T.; Peng, H. L.; Cui, Y. *ACS Nano* **2013**, *7*, 3205.

(11) Tian, B.; Kempa, T. J.; Lieber, C. M. *Chemical Society Reviews* **2009**, *38*, 16.

(12) Wu, Y.; Xiang, J.; Yang, C.; Lu, W.; Lieber, C. M. *Nature* **2004**, *430*, 704.

(13) Lauthon, L. J.; Gudiksen, M. S.; Wang, C. L.; Lieber, C. M. *Nature* **2002**, *420*, 57.

(14) Sciacca, B.; Mann, S. A.; Tichelaar, F. D.; Zandbergen, H. W.; van Huis, M. A.; Garnett, E. C. *Nano Letters* **2014**, *14*, 5891.

(15) Oener, S. Z.; Mann, S. A.; Sciacca, B.; Sfiligoj, C.; Hoang, J.; Garnett, E. C. *Applied Physics Letters* **2015**, *106*, 023501.

(16) Cao, L. Y.; White, J. S.; Park, J. S.; Schuller, J. A.; Clemens, B. M.; Brongersma, M. L. *Nature Materials* **2009**, *8*, 643.

(17) Mann, S. A.; Garnett, E. C. *Nano Letters* **2013**, *13*, 3173.

(18) Garnett, E. C.; Brongersma, M. L.; Cui, Y.; McGehee, M. D. *Annual Review of Materials Research, Vol 41* **2011**, *41*, 269.

(19) Wallentin, J.; Anttu, N.; Asoli, D.; Huffman, M.; Aberg, I.; Magnusson, M. H.; Siefert, G.; Fuss-Kailuweit, P.; Dimroth, F.; Witzigmann, B.; Xu, H. Q.; Samuelson, L.; Deppert, K.; Borgstrom, M. T. *Science* **2013**, *339*, 1057.

(20) Krogstrup, P.; Jorgensen, H. I.; Heiss, M.; Demichel, O.; Holm, J. V.; Aagesen, M.; Nygard, J.; Morral, A. F. I. *Nature Photonics* **2013**, *7*, 306.

(21) Oh, M. H.; Yu, T.; Yu, S. H.; Lim, B.; Ko, K. T.; Willinger, M. G.; Seo, D. H.; Kim, B. H.; Cho, M. G.; Park, J. H.; Kang, K.; Sung, Y. E.; Pinna, N.; Hyeon, T. *Science* **2013**, *340*, 964.

(22) Sun, Y. G.; Xia, Y. N. *Science* **2002**, *298*, 2176.

(23) Li, H. B.; Brescia, R.; Povia, M.; Prato, M.; Bertoni, G.; Manna, L.; Moreels, I. *Journal of the American Chemical Society* **2013**, *135*, 12270.

(24) Beberwyck, B. J.; Alivisatos, A. P. *Journal of the American Chemical Society* **2012**, *134*, 19977.

(25) Son, D. H.; Hughes, S. M.; Yin, Y. D.; Alivisatos, A. P. *Science* **2004**, *306*, 1009.

(26) Zhang, J. T.; Tang, Y.; Lee, K.; Min, O. Y. *Science* **2010**, *327*, 1634.

(27) Li, H. B.; Zanella, M.; Genovese, A.; Povia, M.; Falqui, A.; Giannini, C.; Manna, L. *Nano Letters* **2011**, *11*, 4964.

(28) Cummins, D. R.; Russell, H. B.; Jasinski, J. B.; Menon, M.; Sunara, M. K. *Nano Letters* **2013**, *13*, 2423.

(29) Gonzalez, E.; Arbiol, J.; Puntès, V. F. *Science* **2011**, *334*, 1377.

(30) Park, J.; Zheng, H.; Jun, Y. W.; Alivisatos, A. P. *Journal of the American Chemical Society* **2009**, *131*, 13943.

(31) Yin, Y. D.; Rioux, R. M.; Erdonmez, C. K.; Hughes, S.; Somorjai, G. A.; Alivisatos, A. P. *Science* **2004**, *304*, 711.

(32) Han, S. K.; Gu, C.; Gong, M.; Wang, Z. M.; Yu, S. H. *Small* **2013**, *9*, 3765.

(33) Bai, Y. X.; Yeom, J.; Yang, M.; Cha, S. H.; Sun, K.; Kotov, N. A. *Journal of Physical Chemistry C* **2013**, *117*, 2567.

(34) Zhong, H. Z.; Wang, Z. B.; Bovero, E.; Lu, Z. H.; van Veggel, F. C. J. M.; Scholes, G. D. *Journal of Physical Chemistry C* **2011**, *115*, 12396.

(35) Pryor, W. A. *Journal of the American Chemical Society* **1960**, *82*, 4794.

(36) Pearce, C. I.; Patrick, R. A. D.; Vaughan, D. J.; Henderson, C. M. B.; van der Laan, G. *Geochimica et Cosmochimica Acta* **2006**, *70*, 4635.
(37) Goh, S. W.; Buckley, A. N.; Lamb, R. N.; Rosenberg, R. A.; Moran, D. *Geochimica et Cosmochimica Acta* **2006**, *70*, 2210.
(38) Hung, L. I.; Tsung, C. K.; Huang, W. Y.; Yang, P. D. *Advanced Materials* **2010**, *22*, 1910.

(39) Yin, Y. D.; Erdonmez, C. K.; Cabot, A.; Hughes, S.; Alivisatos, A. P. *Advanced Functional Materials* **2006**, *16*, 1389.
(40) Fan, H. J.; Gosele, U.; Zacharias, M. *Small* **2007**, *3*, 1660.

TOC

